ISSN 1061-933X, Colloid Journal, 2014, Vol. 76, No. 3, pp. 255–270. © Pleiades Publishing, Ltd., 2014.

Micellar Solutions of Ionic Surfactants and Their Mixtures with Nonionic Surfactants: Theoretical Modeling vs. Experiment[1]

P. A. Kralchevsky, K. D. Danov, and S. E. Anachkov

Department of Chemical Engineering, Faculty of Chemistry and Pharmacy, Sofia University
1 James Bourchier Blvd., Sofia, 1164 Bulgaria
e-mail: pk@lcpe.uni-sofia.bg

Received November 11, 2013

Abstract—Here, we review two recent theoretical models in the field of ionic surfactant micelles and discuss the comparison of their predictions with experimental data. The first approach is based on the analysis of the stepwise thinning (stratification) of liquid films formed from micellar solutions. From the experimental stepwise dependence of the film thickness on time, it is possible to determine the micelle aggregation number and charge. The second approach is based on a complete system of equations (a generalized phase separation model), which describes the chemical and mechanical equilibrium of ionic micelles, including the effects of electrostatic and non-electrostatic interactions, and counterion binding. The parameters of this model can be determined by fitting a given set of experimental data, for example, the dependence of the critical micellization concentration on the salt concentration. The model is generalized to mixed solutions of ionic and nonionic surfactants. It quantitatively describes the dependencies of the critical micellization concentration on the composition of the surfactant mixture and on the electrolyte concentration, and predicts the concentrations of the monomers that are in equilibrium with the micelles, as well as the solution's electrolytic conductivity; the micelle composition, aggregation number, ionization degree and surface electric potential. These predictions are in very good agreement with experimental data, including data from stratifying films. The model can find applications for the analysis and quantitative interpretation of the properties of various micellar solutions of ionic surfactants and mixed solutions of ionic and nonionic surfactants.

DOI: 10.1134/S1061933X14030065

1. INTRODUCTION

McBain [1] introduced the term "micelle" (from Latin mica = crumb) into the colloid chemistry to denote surfactant aggregates in aqueous solutions. He suggested that the micelles appear above a particular concentration [2], presently termed "critical micellization concentration" (CMC). The generally accepted model of the spherical micelle was first proposed by Hartley [3]. A review on the early history of the micelle concept can be found in [4].

The first experimental methods applied to study micellar solutions were viscosimetry and conductometry. At present, a variety of other methods are used, such as calorimetry [5]; fluorescence quenching [6]; static and dynamic light scattering [7]; small-angle X-ray scattering [8] and neutron scattering (SANS) [9]; electron paramagnetic resonance [10]; nuclear magnetic resonance [11], and relaxation techniques for studying the micellization dynamics [12].

Two main approaches to the thermodynamics of micellization have been developed. The *mass action model* describes the micellization as a chemical reaction [13, 14]. This model describes the micelles as polydisperse aggregates and allows modeling of the growth of non-spherical micelles and other self-assembled structures [15–19]. The *phase separation model* is focused on the micelle-monomer equilibrium in multi-component surfactant mixtures [14, 20–22]. This model usually works in terms of average aggregation numbers and predicts the CMC, electrolytic conductivity and other properties of mixed surfactant solutions. A detailed review on the thermodynamics of micellization in surfactant solutions was published by Rusanov [23].

Molecular thermodynamic and statistical models of single-component and mixed micelles have been developed [24, 25]. They consider the surfactant molecular structures and give theoretical description of the micellization process based on various free-energy contributions [26, 27]. The CMC values of many nonionic and ionic surfactants have been predicted using the computational quantitative-structure-property-relationship (QSPR) approach [28, 29].

The first models of *micellization kinetics* were developed by Kresheck et al. [30], and Aniansson and Wall [31]. These models have been extended to simultaneously account for the relaxations in the micelle concentration, aggregation number and polydispersity [32]; to predict the dynamic surface tension of micel-

[1] The article is published in the original.

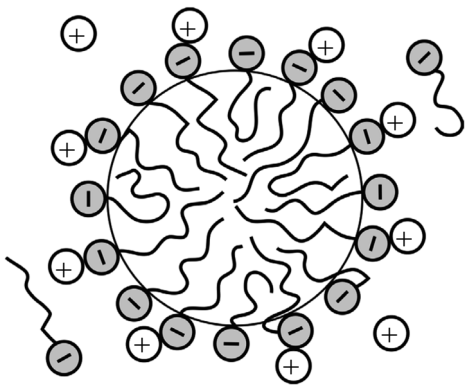

Fig. 1. Sketch of a spherical micelle formed by an anionic surfactant. A part of the surfactant ionizable groups at the micelle surface are neutralized by bound counterions. The rest of the ionizable groups determine the micelle charge, Z.

lar solutions [33–35], and to quantify the micellar relaxation in the case of coexisting spherical and cylindrical micelles [36].

In the present article, we review two recent theoretical models in the field of ionic surfactant micelles and discuss the comparison of their predictions with experimental data. As sketched in Fig. 1, an ionic micelle consists of surfactant ions, bound counterions and of the electric double layer around the micelle. The number of surfactant molecules incorporated in the micelle determines its aggregation number, N_{agg}. The degrees of micelle ionization and counterion binding will be denoted, respectively, by α and θ; at that, $\alpha + \theta = 1$. For simplicity, we will consider monovalent surfactant ions and counterions. The micelle charge (in elementary-electric-charge units) is $Z = \alpha N_{agg}$.

The stepwise thinning (stratification) of foam films formed from solutions of ionic surfactants depends on the micelle aggregation number and charge, N_{agg} and Z. Conversely, from the experimental stratification curves it is possible to determine both N_{agg} and Z with the help of an appropriate theoretical analysis [37, 38]. In addition, information for N_{agg} and Z is "coded" in the experimentally measured dependences (i) of the CMC of ionic surfactant solutions on the concentration of added salt, and (ii) of the solution's electric conductivity on the surfactant concentration. Information for the micellar properties can be extracted by fitting of the experimental curves with a quantitative thermodynamic model that correctly describes the micelle–monomer equilibrium [39].

Section 2 describes the experiments with stratifying films, and the methods for determining N_{agg} and Z from the experimental time-dependencies of the film thickness. Section 3 presents the thermodynamic model of micelle–monomer equilibrium and its application for the analysis of experimental data. Finally, Section 4 is dedicated to the generalization of the thermodynamic model to mixed micellar solutions of ionic and nonionic surfactants. The present review article could be useful for all readers who are interested in the analysis and quantitative interpretation of the properties of micellar solutions containing ionic surfactants.

2. IONIC MICELLES AND STRATIFYING FILMS

2.1. Stepwise Thinning of Liquid Films from Micellar Solutions

The experiments with thin liquid films containing molecules [40] or colloidal spheres [41] indicate the existence of an oscillatory surface force, which is manifested by the stepwise thinning of the films. These effects are due to the ordering of Brownian particles (molecules or colloidal spheres) near the interface. The ordering decays with the distance from the surface. If two interfaces approach each other, the ordered zones near each of them overlap, thus, enhancing the particle ordering within the liquid film [42]. Upon decreasing the film thickness, layers of particles are expelled, one-by-one, which leads to a stepwise thinning (stratification) of the film. This phenomenon was observed long ago by Johonnott [43] and Perrin [44] with films from surfactant solutions and was interpreted by Nikolov et al. [41, 45, 46] as a layer-by-layer thinning of the structure of spherical micelles formed inside the film.

In the case of *nonionic* surfactant micelles, the behavior of the stratifying films can be described in terms of the statistical theory of hard spheres confined between two hard walls [47–51]. In this case, the period of the oscillatory force [50–52] and the height of the stratification step [53–55] is close to the diameter of the nonionic micelle (or another colloidal particle). However, in the case of *ionic* surfactant micelles, the height of the step is considerably greater than the micelle hydrodynamic diameter [37, 38, 41]. Hence, in this case the electrostatic repulsion between the charged micelles determines the distance between them. Following [37, 38], here we will demonstrate that the micelle aggregation number, N_{agg}, and charge, Z can be determined from the stepwise thinning of foam films formed from ionic surfactant solutions.

The most convenient and relatively simple instrument for investigation of stratifying liquid films is the Scheludko–Exerowa (SE) cell [56, 57], which is presented schematically in Fig. 2. The investigated solution is loaded in a cylindrical capillary (of inner diameter $\approx$1 mm) through an orifice in its wall. A biconcave drop is formed inside the capillary. Next, liquid is sucked through the orifice and the two menisci approach each other until a liquid film is formed in the central part of the cell. By injecting or sucking liquid through the orifice, one can vary the radius of the

formed film. Its thickness can be measured by means of an interferometric method [57] of accuracy ±0.5 nm. For this purpose, the light reflected from the film is supplied to a photomultiplier and computer, and the intensity of the reflected light, J, is recorded in the course of the experiment. The film thickness, h, is then determined from the equation [57, 58]:

$$h = \frac{\lambda}{2\pi n}\arcsin\left[\left(\frac{J - J_{\min}}{J_{\max} - J_{\min}}\right)^{1/2}\xi\right], \qquad (1)$$

where λ is the wavelength of the used monochromatic light; n is the mean refractive index of the film; ξ is a correction coefficient for multiple reflection; $J_{\min}$ is the registered intensity of light at broken film, and $J_{\max}$ is the experimentally determined intensity of light reflected from the film at the last interference maximum at $h = \lambda/4n$, which is usually about 100 nm. Equation (1) is valid for films of thickness $h \le \lambda/4n$. The correction coefficient ξ is calculated as follows:

$$\xi = \left[1 + \frac{4\bar{r}^2(1 - \Delta J)}{(1 - \bar{r}^2)^2}\right]^{-1}, \qquad (2)$$

where $\Delta J = (J - J_{\min})/(J_{\max} - J_{\min})$ and $\bar{r} = (n-1)/(n+1)$. For foam films, the refractive index of water is used for n in Eq. (1). The calculated equivalent water thickness h is close to the real thickness of the film.

Figure 3a shows a sketch of a stratifying film that contains ionic surfactant micelles; h_0, h_1, h_2 and h_3 are the thicknesses of portions of the film that contain, respectively, 0, 1, 2 and 3 layers of micelles. Figure 3b shows illustrative experimental data for the stepwise decrease of the film thickness with time for 50 mM aqueous solutions of the anionic surfactant sodium dodecyl sulfate (SDS) and the cationic surfactant cetyl trimethylammonium bromide (CTAB). On the basis of data from many similar experiments, it has been established that the height of the step, $\Delta h = h_n - h_{n-1}$ is independent of n, but decreases with the rise of the ionic surfactant concentration [37, 38]. For 50 mM SDS and CTAB the average values of the step height are, respectively, $\Delta h = 13.7$ and 16.6 nm, whereas the corresponding micelle hydrodynamic diameters are $d_h = 4.5$ and 5.7 nm [37]. As mentioned above, this considerable difference between Δh and d_h is due to the strong electrostatic repulsion between the charged micelles. This effect can be used to determine the properties of the ionic surfactant micelles, viz. N_{agg} can be determined from the experimental Δh, whereas Z can be determined from the final thickness of the film, h_0 (Fig. 3). Note that Δh is simultaneously the height of the step and the period of the oscillatory structural force [42, 50–52, 55].

2.2. Determination of N_{agg} from the Stratification Steps

The theoretical prediction of Δh for films containing charged particles (micelles) demands the use of density-functional-theory calculations and/or Monte Carlo (MC) simulations [59, 60]. However, the theory, simulations and experiments showed that a simple relation exists between Δh and the bulk concentration of micelles, c_m. First, it was experimentally established [41, 45] that the measured values of Δh for foam films from solutions of SDS are practically equal to the average distance, $\delta_l \equiv c_m^{-1/3}$, between two micelles in the bulk of solution, viz.

$$\Delta h \approx \delta_l \equiv c_m^{-1/3} = \left(\frac{c_s - \mathrm{CMC}}{N_{agg}}\right)^{-1/3}. \qquad (3)$$

Here, c_s and CMC are the total input surfactant concentration and the critical micellization concentration expressed as number of molecules per unit volume. The inverse-cubic-root law, $\Delta h \propto c_m^{-1/3}$, was obtained also theoretically [60] and by colloidal probe atomic force microscope (CP-AFM) [61, 62]. The oscillatory surface forces due to the confinement of suspensions of charged nanoparticles between two solid surfaces were investigated theoretically and experimentally in relation to the characteristic distance between the particles in the bulk [63–66]. The bulk suspension was described theoretically by using the integral equations of statistical mechanics in the frame of the hypernetted chain approximation, whereas the bulk structure factor was experimentally determined by SANS [64]. In addition, the surface force of the film was calculated by MC simulations and measured by CP-AFM. In both cases (bulk suspension and thin film) excellent agreement between theory and experiment was established and the obtained results obey the $\Delta h \propto c_m^{-1/3}$ law, where c_m denotes the concentration of charged particles that can be surfactant micelles. Furthermore, it

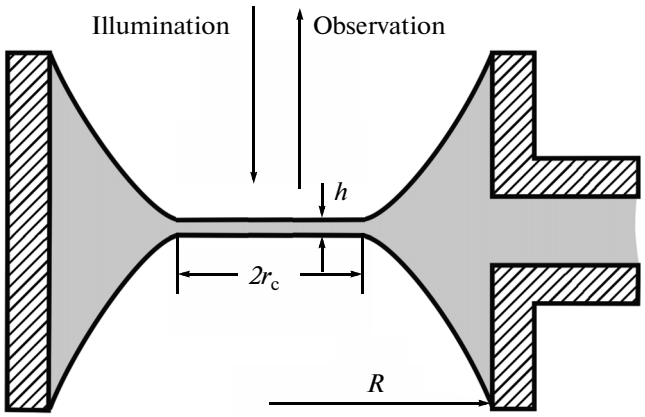

Fig. 2. Cross-section of the SE cell [56, 57] for investigation of thin liquid films. The film of thickness h and radius r_c is formed in the middle of a cylindrical glass capillary of inner radius R. The surfactant solution is loaded in the cell (or sucked out) through an orifice in the capillary wall; details in the text.

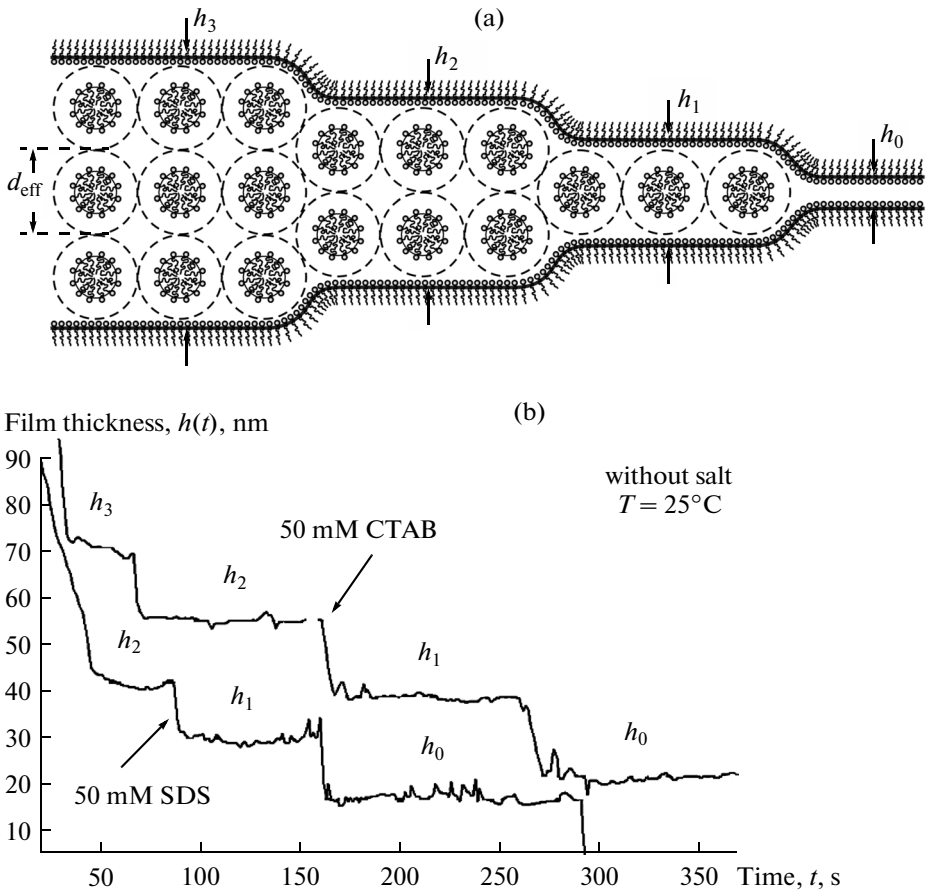

Fig. 3. (a) Sketch of a liquid film from a micellar solution of an ionic surfactant; h_0, h_1, h_2 and h_3 denote the thicknesses of films containing, respectively, 0, 1, 2 and 3 layers of micelles. The height of the step, $\Delta h = h_n - h_{n-1}$ ($n = 1, 2, ...$) is determined by the micelle effective diameter, d_{eff}, which, in its own turn, is determined by the electrostatic repulsion between the micelles. (b) Experimental time dependences of the film thickness, h, for foam films from 50 mM solutions of the ionic surfactants CTAB and SDS formed in a SE cell [37].

was demonstrated that the data obtained with charged particles of different diameters collapse onto a single master curve, $\Delta h = c_m^{-1/3}$ [66]. In other words, the proportionality sign "$\propto$" is replaced with equality sign "=" in agreement with the foam-film experiments [41, 45].

The validity of the empirical $\Delta h = c_m^{-1/3}$ law is limited at low and high particle concentrations, characterized by the effective particle volume fraction (particle + counterion atmosphere) [66]. The decrease of the effective particle volume fraction can be experimentally accomplished not only by dilution, but also by addition of electrolyte that leads to shrinking of the counterion atmosphere [65]. The inverse-cubic-root law, $\Delta h = c_m^{-1/3}$, is fulfilled in a wide range of particle/micelle concentrations that coincides with the range where stratification (step-wise thinning) of free liquid films formed from particle suspension and micellar solution is observed [37, 38, 66].

Because the validity of Eq. (3) has been proven in numerous studies, we can use this equation to determine the aggregation number of ionic surfactant micelles. Solving Eq. (3) with respect to N_{agg}, we obtain [37]:

$$N_{agg} = (c_s - \mathrm{CMC})(\Delta h)^3. \quad (4)$$

Here, c_s and CMC have to be expressed as number of molecules per unit volume. Values of N_{agg} determined from the experimental Δh using Eq. (4) are shown in the table for three ionic surfactants, SDS, CTAB, and cetyl pyridinium chloride (CPC). The micelle aggregation numbers determined in this way compare very well with data for N_{agg} determined by other methods [37, 38].

The table contains also data for the degree of micelle ionization, α, determined as explained in Section 2.4.

2.3. Discussion

The data in the table show that the surfactant with the highest α, SDS, has the smallest aggregation number, N_{agg}. Conversely, the surfactant with the lowest α,

CTAB, has the greatest aggregation number, N_{agg}. Physically, this can be explained with the fact that a greater ionization, α, gives rise to a stronger headgroup repulsion, larger area per headgroup and, consequently, smaller N_{agg}.

Another interesting result in the table refers to the values of micelle charge, Z. Because, the surfactants with greater α have smaller N_{agg}, it turns out that the values of $Z = \alpha N_{agg}$ are not so different; see the table.

The relation $\Delta h = c_m^{-1/3}$, which has been used to determine N_{agg}, can be interpreted as an osmotic-pressure balance between the film and the bulk [37]. The micelles give a considerable contribution to the osmotic pressure of the solution because of the large number of dissociated counterions. The disjoining pressure is approximately equal to the difference between the osmotic pressures in the film and in the bulk: $\Pi \approx P_{osm}(h) - P_{osm}(\infty)$. (The van der Waals component of Π can be neglected for the relatively thick films containing micelles.) Π is a small difference between two much greater quantities, $P_{osm}(h) \approx P_{osm}(\infty)$, under typical experimental conditions. Then, the osmotic pressures of the micelles in the film and in the bulk are approximately equal, and consequently, the respective average micelle concentrations in the film and in the bulk have to be practically the same. Thus, the expulsion of a micellar layer from the film results in a decrease of the film thickness with the mean distance between the micelles in the bulk, as stated by Eq. (3).

As mentioned above, the experimental Δh is significantly greater than the diameter of the ionic micelle. Δh can be considered as an effective diameter of the charged particle, d_{eff}, which includes its counterion atmosphere; see Fig. 3a. A semiempirical expression for calculating Δh was proposed in [37, 38]:

$$d_{eff} = d_h \left\{ 1 + \frac{3}{d_h^3} \int_{d_h}^{\infty} \left[1 - \exp\left(-\frac{3u_{el}(r)}{kT} \right) \right] r^2 \, dr \right\}^{1/3}. \quad (5)$$

Here, d_h is the hydrodynamic diameter of the micelle; k is the Boltzmann constant; T is the absolute temperature, and $u_{el}(r)$ is the energy of electrostatic interaction of two micelles in the solution. The interaction energy $u_{el}(r)$ can be calculated from the expression [37]:

$$\frac{u_{el}(r)}{kT} = \frac{r}{4L_B} \left[\frac{e}{kT} \psi(r/2) \right]^2, \quad (6)$$

where $\psi(r)$ is the distribution of the electrostatic potential around a given ionic micelle in the solution; $L_B \equiv e^2/(4\pi\varepsilon_0\varepsilon kT)$ is the Bjerrum length ($L_B = 0.72$ nm for water at 25°C); ε_0 is the permittivity of vacuum; ε is the dielectric constant of the solvent (water); e is the elementary charge. Equation (6) reduces the two-particle problem to the single-particle problem.

It has been established [37], that d_{eff} calculated from Eqs. (5) and (6) coincides with Δh measured for stratifying films, if $\psi(r)$ is calculated by using the *jellium model* introduced by Beresford-Smith et al. [67, 68]. In this model, the electric field around a given micelle is calculated by assuming Boltzmann distribution of the small ions around the micelle, but *uniform* distribution of the other micelles. In other words, the Debye screening of the electric field of a given micelle in the solution is due only to the small ions (counterions, surfactant monomers and ions of an added salt, if any). The jellium model leads to the following expression for the Debye screening parameter, κ:

$$\kappa^2 = 8\pi L_B I, \quad I = I_b + \frac{1}{2} Z c_m, \quad (7)$$

where I is the ionic strength of the micellar solution; I_b is the ionic strength due to the background electrolyte: I_b = CMC + ionic strength of added salt (if any). The last term in Eq. (7) represents the contribution of the counterions dissociated from the micelles. The jellium model is widely used in the theory of charged particle suspensions and micellar solutions [64, 69, 70].

The relationship $d_{eff} = c_m^{-1/3} = \Delta h$ is satisfied in the whole concentration range where stratifying films are observed; d_{eff} is calculated from Eqs. (5) and (6), and Δh is experimentally determined from the stratification steps, like those in Fig. 3b. In contrast, for $d_{eff} < c_m^{-1/3}$ the foam films do not stratify and the oscillations of dis-

N_{agg}, α and Z determined from the values of Dh and h_0; data from [37, 38]

c_s(mM)	Aggregation number N_{agg} from Eq. (4)	Ionization degree α from Section 4	Charge* Z (e units)
Sodium dodecyl sulfate			
30	48	0.46	22
40	61	0.55	33
50	65	0.53	35
100	65	0.56	37
Cetyl trimethylammonium bromide			
10	95	0.20	19
20	119	0.23	27
30	137	0.26	35
40	136	0.26	35
50	135	0.29	40
Cetyl pyridinium chloride			
10	52	0.30	15
20	75	0.32	24
30	80	0.35	28
40	93	0.36	33
50	93	0.37	34

* The micelle charge is $Z = \alpha N_{agg}$ in elementary-electric-charge units.

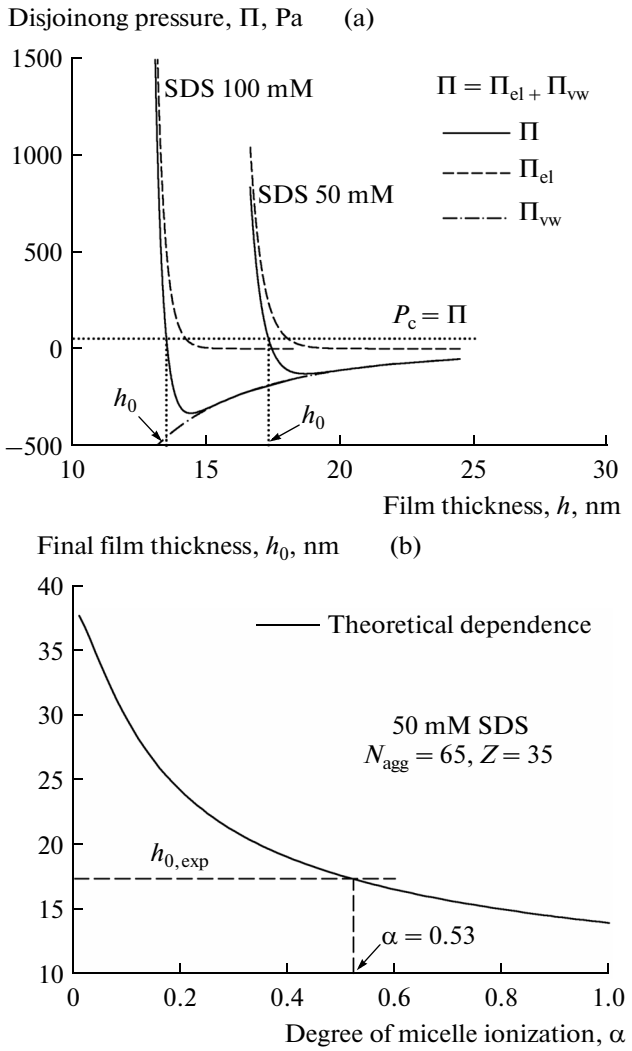

Fig. 4. (a) Plot of the theoretical total disjoining pressure, $\Pi = \Pi_{el} + \Pi_{vw}$, vs. the film thickness, h, where Π_{el} and Π_{vw} are calculated as explained in [38]. The two $\Pi(h)$ curves correspond to 50 and 100 mM SDS. Their intersection points with the horizontal line $\Pi = P_c$ determine the respective theoretical values of h_0. (b) Plot of the determined h_0 (for 50 mM SDS) vs. the micelle ionization degree, α. The intersection point of this theoretical curve with the horizontal line $h_0 = h_{0,exp}$ yields the physical value of α; $h_{0,exp}$ is the experimental value of the final film thickness; details in the text.

joining pressure vanish [37]. This may happen at low micelle concentrations, or at sufficiently high salt concentrations. In the latter case, the Debye screening of the electrostatic interactions is strong, and d_{eff} decreases at the same $c_m^{-1/3}$.

2.4. Determination of the Micelle Charge from h_0

The procedure for determination of the micelle ionization degree, α, and charge, $Z = \alpha N_{agg}$, was proposed and successfully tested in [38]. This procedure is based on the fact that the final film thickness, h_0, depends on α because the counterions dissociated from the micelles in the bulk (i) increase the Debye screening of the electrostatic repulsion and (ii) increase the osmotic pressure of the bulk phase, which leads to a decrease of the film thickness h_0 with the rise of micelle ionization, α. The key step in the procedure is to accurately calculate the theoretical dependence $h_0(\alpha)$. This dependence is obtained from the equation:

$$\Pi(h_0, \alpha) = P_c. \quad (8)$$

As before, Π is the disjoining pressure of the foam film in its final state, which depends on the film thickness, h_0, and on the degree of micelle ionization, α. Equation (8) expresses a condition for mechanical equilibrium of the liquid film stating that the disjoining pressure Π must be equal to the capillary pressure of the adjacent meniscus, P_c [71]. For thin liquid films formed in the SE cell, the capillary pressure P_c can be accurately estimated from the expression [45]:

$$P_c = \frac{2\sigma}{R}(1 - r_c^2/R^2)^{-1}, \quad (9)$$

where σ is the experimental surface tension of the surfactant solution; R and r_c are the cell and film radii (Fig. 2). Expression for the theoretical dependence $\Pi(h_0, \alpha)$ is available and the computational procedure is described in details in [38]. This procedure uses N_{agg} as an input parameter, which is determined from Δh using Eq. (4).

Figure 4a shows the theoretical Π-vs.-h_0 dependencies (corresponding to N_{agg} and α from the table) for solutions with 50 and 100 mM SDS. In accordance with Eq. (8), the intersection point of the $\Pi(h_0)$ curve with the horizontal line $\Pi = P_c$ determines the physical value of h_0. The value of h_0 thus obtained depends on the value of α used to calculate the $\Pi(h_0)$ curve. By varying α, one calculates the theoretical dependence $h_0(\alpha)$, which is shown in Fig. 4b for a foam film formed from 50 mM SDS solution. Finally, the intersection point of the theoretical dependence $h_0(\alpha)$ with the horizontal line $h = h_{0,exp}$ gives the physical value of the ionization degree, α (Fig. 4b). Here, $h_{0,exp}$ is the experimental final film thickness; see Fig. 3. The values of α and of $Z = \alpha N_{agg}$ determined in this way for SDS, CTAB and CPC are given in the table.

The described method for determining N_{agg}, α and Z from the stepwise thinning of foam films from micellar solutions of ionic surfactants (Fig. 3b) has the following advantages. First, N_{agg} and α are determined simultaneously, from the same set of experimental data. Second, N_{agg} and α are obtained at each given surfactant concentration. Third, N_{agg} and α can be determined even for turbid solutions, like those of carboxylates, where the micelles coexist with crystallites and the light-scattering and fluorescence methods are inapplicable [38]. In Section 3.5, values of N_{agg} and α

determined in this way are compared with data obtained (completely independently) from the fit of the experimental CMC-vs.-salt-concentration dependence by a generalized phase-separation model [39].

3. THE GENERALIZED PHASE SEPARATION MODEL

3.1. The Chemical Equilibrium between Micelles and Free Monomers

The "phase separation" models of micellization [14, 72] are based on the condition for chemical equilibrium between monomers and micelles, which states that the chemical potentials of a molecule from a given component as a free monomer, and as a constituent of a micelle, must be equal:

$$\mu_i^{(w,0)} + kT\ln(\gamma_i c_i) = \mu_i^{(mic,0)} + kT\ln(f_i y_i). \qquad (10)$$

Here, the subscript i numerates the components; $\mu_i^{(w,0)}$ is the standard chemical potential of a free monomer in the water phase; c_i and γ_i are the respective bulk concentration and activity coefficient. Likewise, $\mu_i^{(mic,0)}$ is the standard chemical potential of the molecule in the micelles; y_i and f_i are the respective molar fraction and activity coefficient. In the phase separation models, the micelles are considered as quasi-monodisperse, i.e., $\mu_i^{(mic,0)}$, y_i and f_i are assumed to be average values. A basic parameter of the model is the micellization constant, $K_i^{(mic)}$, which is related to the difference between the standard chemical potentials in Eq. (10):

$$\ln K_i^{(mic)} = [\mu_i^{(mic,0)} - \mu_i^{(w,0)}]/kT. \qquad (11)$$

$\ln K_i^{(mic)}$ expresses the change of the standard free energy (in kT units) upon the transfer of a free surfactant monomer from the bulk into the micelle. For *nonionic* surfactants, the following simple relation holds [72]:

$$K_i^{(mic)} = \mathrm{CMC}_i, \qquad (12)$$

where CMC_i is the critical micellization concentration for the *pure* component i.

For *ionic* surfactants, the model (Section 3.2) is more complicated. It allows one to predict the CMC of ionic micelles at various salt concentrations; the CMC of mixed micelles from ionic and nonionic surfactants as a function of composition; the composition of monomers that are in equilibrium with the micelles; the degree of counterion binding; the micelle aggregation number, charge and surface electric potential, and the electrolytic conductivity of the micellar solutions [39].

3.2. The Complete System of Equations

For simplicity, let us focus on micellar solutions of a single ionic surfactant, which represents 1 : 1 electrolyte. Such solution contains at least two components, viz. surfactant ions and counterions, which will be denoted with subscripts 1 and 2, respectively. It is assumed that the solution may also contain non-amphiphilic electrolyte (salt) with the same counterions as the surfactant. The complete system of equations includes chemical-equilibrium relationships, like Eq. (10), mass balance equations, expressions for the activity coefficient, $\gamma_\pm$, etc. Here, we will first give the equations of the system, following [39], and then we will separately discuss the physical meaning of each equation:

$$\ln(c_1\gamma_\pm) = \ln K_1^{(mic)} + \ln y_1 + \Phi_s, \qquad (13)$$

$$\ln c_{12} = \ln K_1^{(mic)} + \ln y_2, \qquad (14)$$

$$c_{12} = K_{St} c_1 c_2 \gamma_\pm^2, \qquad (15)$$

$$y_1 + y_2 = 1, \qquad (16)$$

$$c_1 + c_{12} + c_{mic} = C_1, \qquad (17)$$

$$c_2 + c_{12} + y_2 c_{mic} = C_1 + C_{salt}, \qquad (18)$$

$$\log\gamma_\pm = -\frac{A\sqrt{I}}{1 + Bd_i\sqrt{I}} + bI, \qquad (19)$$

$$I = \frac{1}{2}(c_1 + c_2 + C_{salt}). \qquad (20)$$

$\Phi_s = e|\psi_s|/kT$ is the dimensionless micelle surface electric potential; e is the elementary electric charge and ψ_s is the dimensional surface potential; c_1 and c_2 are the bulk concentrations of free surfactant ions and counterions (e.g., in the case of SDS, c_1 and c_2 are the concentrations of free DS^- and Na^+ ions); c_{12} is the concentration of free non-ionized surfactant molecules in the bulk; y_1 and y_2 are the molar fractions of the ionized and non-ionized surfactant molecules in the micelles (Fig. 1); C_1 and C_{salt} are the total concentrations of dissolved surfactant and salt; c_{mic} is the number of surfactant molecules in micellar form per unit volume of the solution; I is the solution's ionic strength; $K_1^{(mic)}$ is the micellization constant of the ionic surfactant, see Eq. (11); K_{St} is the Stern constant characterizing the counterion binding to the surfactant headgroups. (Here, we consider the terms counterion binding, condensation and adsorption as synonyms.)

A, Bd_i and b are parameters in the semiempirical expression, Eq. (19), for the activity coefficient $\gamma_\pm$ originating from the Debye–Hückel theory. Their values at 25°C, obtained by fitting data for $\gamma_\pm$ of NaCl and NaBr from [73] by Eq. (19), are $A = 0.5115\ \mathrm{M}^{-1/2}$, $Bd_i = 1.316\ \mathrm{M}^{-1/2}$ and $b = 0.055\ \mathrm{M}^{-1}$. These values can be used also for solutions of other alkali metal halides.

The physical meaning of Eqs. (13)–(20) is as follows. Equations (13) and (14) express the chemical equilibrium between monomers and micelles with respect to the surfactant ions and non-ionized surfactant molecules, respectively. In the latter case, the

incorporation of non-ionized surfactant molecules in the micelles is thermodynamically equivalent to counterion binding to the surfactant headgroups at the micelle surface. In a closed system, the final equilibrium state is independent of the reaction path [74]. From this viewpoint, the equilibrium state of the system should be independent of whether (i) the association of surfactant ion and counterion happens in the bulk, and then non-ionized surfactant molecules are incorporated in the micelles, or (ii) ionized surfactant molecules are first incorporated in the micelles, and afterwards, counterions bind to their headgroups. As in [39], the term "non-ionized" surfactant molecules is used for both non-dissociated molecules (such as protonated fatty acids) and solvent-shared (hydrated) ion pairs [75] of surfactant ion and counterion. Equation (15) expresses the respective bulk association–dissociation equilibrium relationship.

Equation (16) is the known identity relating the molar fractions, y_1 and y_2, of the ionized and non-ionized surfactant molecules in the micelle (Fig. 1). Equations (17) and (18) express, respectively, the mass balance of the surfactant (component 1) and counterion (component 2). As mentioned above, the surfactant and salt are assumed to have the same counterions (e.g., Na^+ ions for SDS and NaCl). Equation (17) is the semiempirical expression for the activity coefficient (see above), and Eq. (20) expresses the ionic strength, I, of the micellar solution. In Section 3.3, we demonstrate that Eq. (20) follows from the jellium model, Eq. (7), and the condition for electroneutrality of the solution.

Equations (13)–(20) represent a system of 8 equations that contains 9 unknown variables: c_1, c_{12}, c_2, c_{mic}, y_1, y_2, $\gamma_\pm$, I, and Φ_s. Hence, we need an additional equation to close the system. Different possible closures were verified [39]. The best results were obtained with an equation proposed by Mitchell and Ninham [76]. This equation states that the repulsive electrostatic surface pressure, due to the charged surfactant headgroups at the micelle surface, π_{el}, is exactly counterbalanced by the non-electrostatic component of the micelle surface tension, γ_0, that is $\pi_{el} = \gamma_0$. Physically, γ_0 is determined by the net lateral attractive force due to the cohesion between the surfactant hydrocarbon tails, and to the hydrophobic effect in the contact zone tail/water at the micelle surface. Hence, γ_0 is expected to be independent of the bulk surfactant and salt concentrations, i.e. $\gamma_0 = \text{const}$.

The equation $\pi_{el} = \gamma_0$ expresses a lateral mechanical balance of attractive and repulsive forces in the surface of charges, i.e. in the surface where the micelle surface charges are located. This equation can be expressed also in the form $\gamma_0 + \gamma_{el} = 0$, where $\gamma_{el} = -\pi_{el}$ is the electrostatic component of the micelle surface tension. In other words, the considered equation means that the micelle is in a *tension-free state*. The term "tension free state" was introduced by Evans and Skalak [77] in mechanics of phospholipid bilayers and biological membranes. Physically, zero tension means that the acting lateral repulsive and attractive forces counterbalance each other.

Using the theory of the electric double layer, Mitchell and Ninham derived an expression for π_{el}, which was set equal to γ_0. For a spherical micelle of radius R_m at the CMC, the result reads [76]:

$$8\varepsilon\varepsilon_0\kappa\left(\frac{kT}{e}\right)^2 \times \left\{\sinh^2\left(\frac{\Phi_s}{4}\right) + \frac{2}{\kappa R_m}\ln\left[\cosh\left(\frac{\Phi_s}{4}\right)\right]\right\} = \gamma_0. \quad (21a)$$

Here, ε_0 is the dielectric permittivity of vacuum; ε is the relative dielectric constant of solvent (water); κ is the Debye screening length and R_m is the radius of the surface of charges for the micelle; γ_0 is presumed to be constant and represents one of the parameters of the model characterizing a given ionic surfactant. Equation (21a) is appropriate for interpreting the dependence of the CMC on the concentration of added salt (see below). The left-hand side of Eq. (21a) represents a truncated series expansion for large κR_m.

At concentrations above the CMC, the counterions dissociated from the micelles essentially contribute to the Debye screening of the electrostatic interactions in the solution. The Mitchell–Ninham closure, Eq. (21a) can be generalized for surfactant concentrations ≥CMC, as follows [39]:

$$\gamma_0 = \pi_{el} = 8\varepsilon\varepsilon_0\kappa\left(\frac{kT}{e}\right)^2\left\{H(\Phi_s)\sinh^2\left(\frac{\Phi_s}{4}\right) - \frac{\nu\Phi_s}{4}\frac{\frac{\Phi_s}{4} - \tanh\left(\frac{\Phi_s}{4}\right)}{H(\Phi_s)\sinh\left(\frac{\Phi_s}{2}\right)} + \frac{2}{\kappa R_m}\ln\left[\cosh\left(\frac{\Phi_s}{4}\right)\right]\right\}. \quad (21b)$$

Equation (21b) also represents a truncated series expansion for large κR_m, where

$$H(\Phi_s) \equiv \left[\frac{G(\Phi_s)}{\cosh(\Phi_s) - 1}\right]^{1/2}, \quad (22)$$

$$G(\Phi_s) \equiv \cosh\Phi_s - 1 + \nu(\sinh\Phi_s - \Phi_s), \quad (23)$$

$$\nu \equiv \frac{Zc_m}{2(c_1 + C_{salt}) + Zc_m} = \frac{y_1 c_{mic}}{2I} < 1. \quad (24)$$

The relation $Zc_m = y_1 c_{mic}$ has been used. At the CMC ($c_m \to 0$), we have $\nu \to 0$, $H \to 1$, and Eq. (21b) reduces to Eq. (21a). The more general Eq. (21b) has to be used when interpreting data for the electrolytic conductivity of micellar solutions at concentrations above the CMC (see below).

Equations (13)–(21) form a *complete system* of equations for determining the nine unknown variables, c_1, c_{12}, c_2, c_{mic}, y_1, y_2, $\gamma_\pm$, I, and Φ_s. For Eq. (21),

one can use Eq. (21a) for $C_1 = \mathrm{CMC}$ and Eq. (21b) for $C_1 \geq \mathrm{CMC}$. Because the concentrations may vary by orders of magnitude, the numerical procedure for solving this system of equations is non-trivial. An appropriate computational procedure has been developed in [39].

The system of Eqs. (13)–(21) contains only three unknown material parameters, which can be determined from fits of experimental data; these are the micellization constant $K_1^{(\mathrm{mic})}$; the non-electrostatic component of the micelle surface tension, γ_0, and the Stern constant of counterion binding, K_{St}. Note that K_{St} can be independently determined by fit of surface tension data for the respective surfactant; see e.g. [35, 37].

3.3. Discussion on the Basic Equations

If Eq. (13) is subtracted from Eq. (14), and c_{12} is eliminated from Eq. (15), one obtains:

$$\frac{y_2}{y_1} = K_{\mathrm{St}}\gamma_{\pm}c_2\exp(\Phi_s). \tag{25}$$

Equation (25) represents a form of the Stern isotherm of counterion binding to the surfactant headgroups at the micelle surface. In other words, the Stern isotherm is a corollary from the equations of the basic system, Eqs. (13)–(21). This fact mathematically expresses the thermodynamic principle that the final equilibrium state is independent of the reaction path; in our case, of whether the association of surfactant ion and counterion happens in the bulk or at the micelle surface (see above).

Next, let us discuss the expression for the ionic strength, I, of the micellar solution. In the framework of the *jellium model* [67, 68], which has been successfully tested in many studies, the ionic strength is:

$$I = c_1 + C_{\mathrm{salt}} + \frac{1}{2}y_1c_{\mathrm{mic}}. \tag{26}$$

The first two terms, $c_1 + C_{\mathrm{salt}}$, represent the contributions from the ionic surfactant monomers and the added salt. The last term expresses the contribution of the counterions dissociated from the micelles. In addition, the *electroneutrality* of the solution leads to the relationship:

$$c_2 = c_1 + C_{\mathrm{salt}} + y_1c_{\mathrm{mic}}. \tag{27}$$

Here, the counterion concentration, c_2, includes contributions from the dissociated surfactant monomers, molecules of salt, and micelles. Formally, Eq. (27) can be derived by subtracting Eq. (17) from Eq. (18), so that it is not an independent equation from the viewpoint of the system of Eqs. (13)–(21). The elimination of y_1c_{mic} between Eqs. (26) and (27) yields Eq. (20) for the ionic strength of the micellar solution, I. Hence, in view of the electroneutrality condition, Eq. (27), the expression of I by Eq. (20) is equivalent to the respective expression of the jellium model, Eq. (26).

At given $K_1^{(\mathrm{mic})}$, K_{St} and γ_0, the solution of the system, Eqs. (13)–(21), gives the concentrations of all species in the bulk: c_1, c_{12}, c_2, and c_{mic}; the composition of the micelle: y_1 and y_2, and the micelle surface potential Φ_s. The degree of micelle ionization is $\alpha = y_1$, whereas the degree of counterion binding at the micelle surface is $\theta = 1 - \alpha = y_2$. Next, one can calculate the number of surfactant headgroups per unit area of the surface of charges:

$$\frac{N_{\mathrm{agg}}}{A_{\mathrm{m}}} = \Gamma_1, \tag{28}$$

where, as usual, N_{agg} is the micelle aggregation number, and A_{m} is the micelle surface area. Γ_1 can be calculated from the relation between the surface electric potential, Φ_s, and the surface charge density, $y_1\Gamma_1$, originating from the electric-double-layer theory [39]:

$$\frac{\kappa y_1\Gamma_1}{4I} \approx 2\sinh\left(\frac{\Phi_s}{2}\right)\left[\frac{G(\Phi_s)}{\cosh\Phi_s - 1}\right]^{1/2} + \frac{4}{\kappa R_{\mathrm{m}}}\left\{\tanh\left(\frac{\Phi_s}{4}\right) - \frac{\nu\Phi_s}{G(\Phi_s)}\left[\frac{\Phi_s}{4} - \tanh\left(\frac{\Phi_s}{4}\right)\right]\right\}, \tag{29}$$

where $G(\Phi_s)$ and ν are defined by Eqs. (23) and (24). (Higher-order terms in the expansions for $\kappa R_{\mathrm{m}} \gg 1$ have been neglected.) At the CMC, the micelle concentration is negligible; then $\nu \to 0$ and Eq. (29) reduces to a simpler expression derived in Refs. [76, 78]:

$$\frac{\kappa y_1\Gamma_1}{4I} \approx 2\sinh\left(\frac{\Phi_s}{2}\right) + \frac{4}{\kappa R_{\mathrm{m}}}\tanh\left(\frac{\Phi_s}{4}\right). \tag{29a}$$

The second term $\propto 1/(\kappa R_{\mathrm{m}})$ in Eqs. (29) and (29a), that accounts for the surface curvature of the micelle, is always a small correction. Indeed, at the *higher* surfactant concentrations we have $1/(\kappa R_{\mathrm{m}}) \ll 1$. In addition, Φ_s is greater at the *lower* surfactant concentrations, where $\sinh(\Phi_s/2) \gg \tanh(\Phi_s/4)$, so that the first term in the right-hand side of Eq. (29a) is predominant again. Equations (29) and (29a) are approximate expressions, because they take the curvature effect as a first order approximation, but the curvature correction term is always small, so that these two equations give Γ_1 with a very good accuracy [39].

Thus, the solution of the basic system, Eqs. (13)–(21), along with Eq. (29) or (29a), yields Γ_1. Next, for a spherical micelle of radius R_{m}, we have $A_{\mathrm{m}} = 4\pi R_{\mathrm{m}}^2$, and from Eq. (28) we determine the micelle aggregation number N_{agg}. Finally, the micelle charge is $Z = y_1N_{\mathrm{agg}}$.

3.4. Interpretation of the Corrin–Harkins Plot

In 1947, Corrin and Harkins [79] showed that the dependence of CMC of the ionic surfactants on the

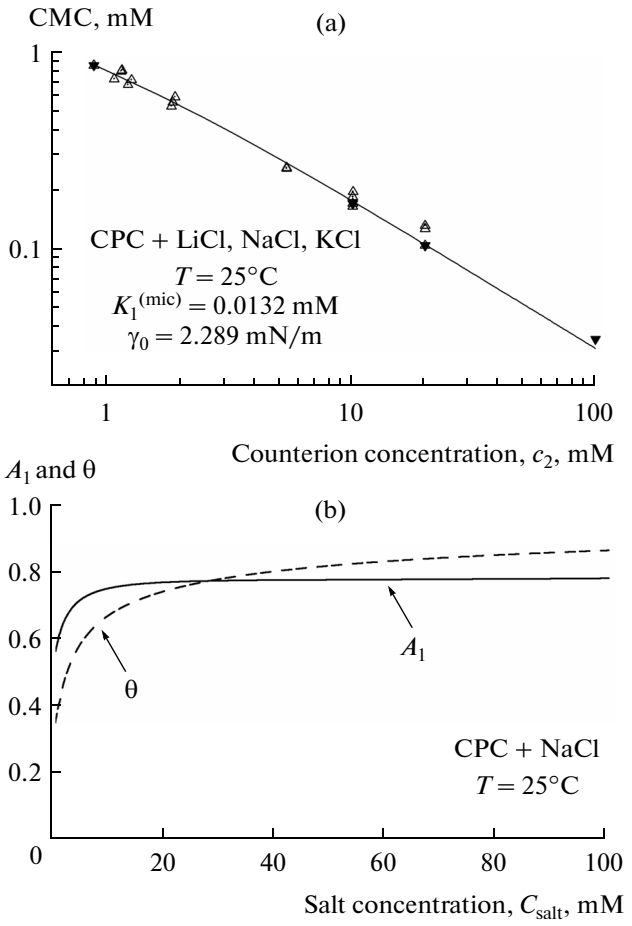

Fig. 5. (a) Plot of the CMC of CPC vs. the counterion concentration at different concentrations of added salt: data from [37, 80]; the solid line is the best fit corresponding to $K_1^{(mic)} = 0.0132$ mM and $\gamma_0 = 2.289$ mN/m. (b) Plot of the running slope of the best-fit line, A_1, and of the degree of counterion binging, $\theta = y_2$ vs. the NaCl concentration; A_1 and θ are calculated by solving the system of Eqs. (13)–(21) and using Eq. (31).

solution's ionic strength I becomes (almost) linear when plotted in double logarithmic scale:

$$\log CMC = A_0 - A_1 \log I, \qquad (30)$$

A_0 and A_1 are constant coefficients. For 1 : 1 electrolytes, at the CMC the ionic strength coincides with the concentration of counterions: $I = c_2 = c_1 + C_{salt}$. As an illustrative example, Fig. 5a shows the plot of data for CPC from [37, 80] in accordance with Eq. (30).

Corrin [81] interpreted A_1 as the degree of counterion binding, i.e. as the occupancy of the micellar Stern layer by adsorbed counterions $\theta = 1 - \alpha$. Because Eqs. (13)–(21) represent a complete system of equations, they allow one to calculate the derivative

$$A_1 = \frac{d\log CMC}{d\log I}, \qquad (31)$$

and to compare the result with $\theta = y_2$. Thus, we could verify whether really A_1 is equal to θ. Explicit expression for A_1 can be found in [39].

For the specific case of CPC, values $K_{St} = 5.93$ M^{-1} and $R_m = 2.58$ nm have been obtained in [37]. Next, the data in Fig. 5a have been fitted with the model based on Eqs. (13)–(21), and the other two parameters have been determined from the best fit, viz. $K_1^{(mic)} = 0.0132$ mM and $\gamma_0 = 2.289$ mN/m. The computational procedure is described in [39].

The solid line in Fig. 5a shows the best fit; one sees that the dependence has a noticeable curvature, although it is close to a straight line. This is better illustrated in Fig. 5b, where the dependencies of A_1, from Eq. (31), and $\theta = y_2$ corresponding to the best fit are plotted vs. C_{salt}. The degree of counterion binding, $\theta = y_2$, is lower than A_1 at the lower salt concentrations (Fig. 5b). Thus, at $C_{salt} = 0$ we have $\theta = 0.34$, whereas $A_1 = 0.55$. Conversely, at the higher salt concentrations the calculations give $y_2 > A_1$. For example, at $C_{salt} = 100$ mM we have $\theta = 0.85$, whereas $A_1 = 0.77$.

In summary, the comparison of the generalized phase-separation model, based on Eqs. (13)–(21), with experimental Corrin–Harkins plots leads to the following conclusions: (i) The Corrin–Harkins plot is not a perfect straight line. (ii) In general, its slope, A_1, is different from the degree of counterion binding, θ; we could have either $A_1 > \theta$ or $A_1 < \theta$ depending on the surfactant concentrations. (iii) The fit of the experimental Corrin–Harkins plot allows one to determine the parameters $K_1^{(mic)}$ and γ_0 of the generalized phase-separation model. These conclusions are based not only on the fit of data for CPC, but also for other ionic surfactants in [39].

3.5. Test of the Theory against Data for N_{agg}, α and Conductivity

Having determined the parameters of the model (see Section 3.4), we are able to predict the micelle aggregation number and ionization degree, N_{agg} and α, as well as all other parameters of the model, based on Eqs. (13)–(21). As an example, the solid and dashed lines in Fig. 6a show the calculated dependencies of N_{agg} and α on the CPC concentration, C_1, without added salt. N_{agg} is calculated from Eqs. (28) and (29) assuming spherical micelles $A_m = 4\pi R_m^2$. In the concentration range $10 \le C_1 \le 50$ mM CPC, the calculated N_{agg} increases from 53 to 99, whereas α decreases from 0.42 to 0.28.

The symbols in Fig. 6a show data for N_{agg} and α from the table, which have been determined completely independently from the stepwise thinning of foam films from CPC solutions. The theoretical lines in the same figure are drawn substituting the indepen-

dently determined values of the parameters K_{St}, $K_1^{(mic)}$ and γ_0; see Section 3.4. In other words, the theoretical lines in Fig. 6a are drawn without using any adjustable parameters. The good agreement between these curves and the experimental points confirms the correctness of the generalized phase-separation model from Section 3.2 [39].

Figure 6b shows a set of experimental data for the electrolytic conductivity κ_e for CPC solutions from [37]. The CMC appears as a kink in the conductivity vs. surfactant concentration plot. The following equation can be used for the quantitative interpretation of conductivity [82, 83]:

$$\kappa_e = \kappa_0 + \lambda_1^{(0)} c_1 + \lambda_2^{(0)} c_2 + \lambda_{co}^{(0)} C_{salt} + Z\lambda_m c_m - AI^{3/2} + BI^2. \quad (32)$$

Here, $\lambda_1^{(0)}$, $\lambda_2^{(0)}$ and $\lambda_{co}^{(0)}$ are the limiting (at infinite dilution) molar conductances, respectively, of the surfactant ions, counterions and coions due to the non-amphiphilic salt (if any). Here, it is assumed that all electrolytes (except the micelles) are of 1 : 1 type. Values of the limiting molar conductances of various ions can be found in handbooks [84, 85]. The term $Z\lambda_m c_m$ accounts for the contribution of the micelles to the conductivity κ_e; λ_m stands for the molar conductance of the micelles; as before, c_m and Z are the micelle concentration and charge. The constant term κ_0 accounts for the presence of a background electrolyte in the water used to prepare the solution. Usually, κ_0 is due to the dissolution of a small amount of CO_2 from the atmosphere; κ_0 has to be determined as an adjustable parameter. The last two terms of Eq. (32) present an empirical correction (the complemented Kohlrausch law) that accounts for long-range interactions between the ions in the aqueous solution. It was experimentally established that the constant parameters A and B are not sensitive to the type of 1 : 1 electrolyte [82, 83].

At $C_1 < CMC$, the data for conductivity κ_e of CPC solutions in Fig. 6b are fitted by means of Eq. (32) with $c_m = 0$ and $I = c_2 = C_1 + C_{salt}$. Two parameters, $\lambda_1^{(0)} = 19.5 \pm 0.1$ cm^{2}S/mol and $\kappa_0 = 0.002 \pm 0.0002$ mS/cm, have been determined from this fit. The investigated CPC sample contains an admixture of 0.08 mol % NaCl, which has been taken into account.

At $C_1 > CMC$ the theoretical curve for κ_e in Fig. 6b is calculated using Eq. (32) with $\lambda_m = 0$ and with known values of all other parameters (no adjustable parameters). The calculated line excellently agrees with the experimental data, indicating that *the micelles give no contribution to the conductivity* κ_e as carriers of electric current. The same result was obtained also for solutions of other ionic surfactants in [39]. This result calls for discussion.

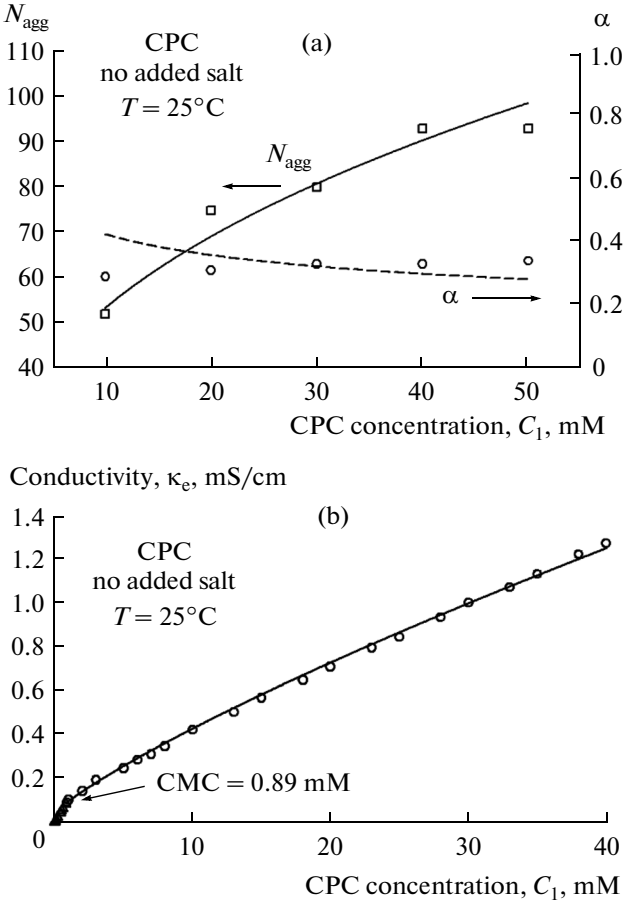

Fig. 6. Test of the theory against data for micellar solutions of CPC. (a) Micelle aggregation number, N_{agg}, and ionization degree, α, vs. C_1: the points are from table; the lines are calculated by solving the system of Eqs. (13)–(21) with $K_1^{(mic)}$ and γ_0 from Fig. 5a; no adjustable parameters. (b) Electrolytic conductivity vs. C_1: the experimental points are from [37]; at $C_1 > CMC$, the solid line is the theoretical curve drawn according to Eq. (32) with $\lambda_m = 0$; details in the text.

The quantitative analysis of the conductivity data in [39] unambiguously yields λ_m identically equal to zero in the whole range of investigated surfactant concentrations. In other words, the conductivity is solely due to the small ions, viz. the free counterions, the surfactant monomers, and the ions of the added salt. The micelles contribute to the conductivity only indirectly, through the counterions dissociated from their surfaces.

One possible hypothesis for explaining the result $\lambda_m = 0$, which was proposed and confirmed in [39], is the following. The electric repulsion between a given micelle and its neighbors is so strong that it can counterbalance the effect of the applied external electric field, which is unable to bring the micelles into directional motion as carriers of electric current. This inter-

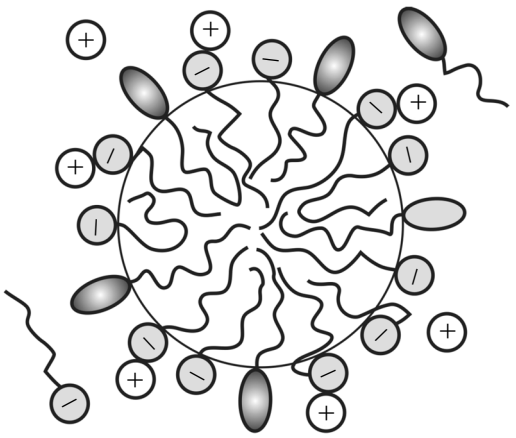

Fig. 7. Sketch of a mixed micelle of an anionic and a nonionic surfactant. A part of the anionic headgroups is neutralized by bound counterions.

micellar repulsion is the same that determines d_{eff} in Fig. 3a and the heights of the steps in Fig. 3b.

A simplified model with constant N_{agg}, α and c_1 is often used to determine the micelle ionization degree α by interpretation of conductivity data, κ_e vs. C_1, at concentrations above the CMC; see e.g. Ref. [86]. In the framework of the simplified model, the micellar term in Eq. (32) is expressed in the form:

$$Z\lambda_m c_m = \frac{\alpha^2 N_{\text{agg}} e^2 N_A}{6\pi\eta R}(C_1 - \text{CMC}), \qquad (33)$$

where N_A is the Avogadro number; C_1 and CMC are to be substituted in moles/m^3; $1/(6\pi\eta R)$ is the hydrodynamic mobility of the ions according to Stokes [82] with η being the viscosity of water; the following relations have been also used: $Z = \alpha N_{\text{agg}}$ and $c_m = (C_1 - \text{CMC})/N_{\text{agg}}$. Further, an average value of N_{agg} is taken from another experiment or from molecular-size estimate, and the dependence of κ_e on C_1 above the CMC (see Fig. 6b) is fitted with a linear regression and α in Eq. (33) is determined as an adjustable parameter from the slope.

Thus, the simplified model gives a constant value of α for the whole concentration domain above the CMC. This constant value is $\alpha = 0.21$, calculated with $N_{\text{agg}} = 75$ for CPC micelles [37]. It is considerably smaller than α calculated using the detailed model, which varies in the range 0.28–0.66 (Fig. 6a). These results illustrate the fact that the simplified model gives systematically smaller values of α than the detailed model. The origin of this difference is the following:

In the simplified model, it is presumed that λ_m gives a finite contribution to κ_e, see Eq. (33), and a part of the electric current is carried by the micelles. Then, to get the same experimental conductivity, κ_e, it is necessary to have a lower concentration of dissociated counterions. As a result, the fit of the conductivity using Eq. (33) leads to a lower degree of micelle ionization α determined as an adjustable parameter.

In the detailed model, using the calculated concentrations of all monomeric ionic species, we predicted their total conductivity, which turned out to exactly coincide with the experimentally measured conductivity, κ_e, in the whole range of surfactant concentrations above the CMC. In other words, there is nothing left for the micelles, so that their equivalent conductance, λ_m, turns out to be zero (or negligible).

Finally, it should be noted that a generalization of the model to the case of one ionic surfactant with several different kinds of counterions is available in [39].

4. MIXED MICELLAR SOLUTIONS OF IONIC AND NONIONIC SURFACTANTS

4.1. The Complete System of Equations

The model for ionic surfactants from Section 3.2 can be extended to the case of mixed solutions of ionic and nonionic surfactant, which may contain also added salt [39]. In this case, two additional variables appear: the concentration of nonionic surfactant monomers, c_n, and the molar fraction of this surfactant in the micelles, y_n. To determine these two variables, we have to include two additional equations in the system of Eqs. (13)–(21). In general, the interaction of the two components in the mixed micelles (Fig. 7) should be taken into account by introducing micellar activity coefficients, f_1 and f_2. For reader's convenience, here we first give the complete system of equations for a mixed solution of an ionic and a nonionic surfactant from [39], and then the differences with respect to Section 3.2 are discussed:

$$\ln(c_1\gamma_\pm) = \ln K_1^{(\text{mic})} + \ln f_1 y_1 + \Phi_s, \qquad (34)$$

$$\ln c_{12} = \ln K_1^{(\text{mic})} + \ln f_1 y_2, \qquad (35)$$

$$c_{12} = K_{\text{St}} c_1 c_2 \gamma_\pm^2, \qquad (36)$$

$$y_1 + y_2 + y_n = 1, \qquad (37)$$

$$c_1 + c_{12} + (y_1 + y_2)c_{\text{mic}} = C_1, \qquad (38)$$

$$c_2 + c_{12} + y_2 c_{\text{mic}} = C_1 + C_{\text{salt}}, \qquad (39)$$

$$\log\gamma_\pm = -\frac{A\sqrt{I}}{1 + Bd_i\sqrt{I}} + bI, \qquad (40)$$

$$I = \frac{1}{2}(c_1 + c_2 + C_{\text{salt}}), \qquad (41)$$

$$\pi_{el}(\kappa, \Phi_s) = f_1 y_1 \gamma_{1,0}, \qquad (42)$$

$$\ln c_n = \ln K_n^{(\text{mic})} + \ln(f_n y_n), \qquad (43)$$

$$c_n + y_n c_{\text{mic}} = C_n. \qquad (44)$$

The function $\pi_{el}(\kappa, \Phi_s)$ in Eq. (42) is equal to the left-hand side of Eq. (21a) or (21b), respectively, at $C_1 = \text{CMC}$ and $C_1 \geq \text{CMC}$; $\gamma_{1,0}$ equals the non-electrostatic

component of the surface tension γ_0 for a micelle from the ionic component 1 alone, which can be determined from a fit like that in Fig. 5a. The micellar activity coefficients f_1 and f_2 can be expressed from the regular solution theory [87]:

$$f_1 = \exp(\beta y_n^2), \quad f_n = \exp[\beta(1-y_n)^2]. \qquad (45)$$

β is an additional parameter of the model that characterizes the interactions between the two surfactant components in the micelle, and which is liable to determination as an adjustable parameter from fits of experimental data (see below).

Equations (34)–(42) are counterparts of Eqs. (13)–(21) in the case of single ionic surfactant. The differences are that Eqs. (34) and (35) contain the activity coefficient f_1; Eq. (37) includes the molar fraction of the nonionic surfactant, y_n; Eq. (38) accounts for the fact that now the sum $y_1 + y_2$ is not equal to 1; Eq. (42) takes into account that only the ionic surfactant contributes to the electrostatic surface pressure of the mixed micelle, π_{el}; Eq. (43) expresses the chemical equilibrium between micelles and monomers with respect to exchange of the nonionic surfactant, and finally, Eq. (44) expresses the mass balance of the nonionic surfactant.

Equations (34)–(45) represent a complete system of equations for determining the 13 unknown variables: c_1, c_{12}, c_2, c_n, c_{mic}, y_1, y_2, y_n, f_1, f_n, $\gamma_\pm$, I, and Φ_s. This system contains only 5 thermodynamic parameters: K_{St}, $K_1^{(mic)}$, $\gamma_{1,0}$, $K_n^{(mic)}$ and β. The first three of them characterize the ionic surfactant; they have been already determined for a number of ionic surfactants – see Table 3 in [39]; for CPC – see Section 3.4 above. $K_n^{(mic)}$ equals the CMC of the pure nonionic surfactant, see Eq. (12), which is known from the experiment. Then, only the interaction parameter β, which characterizes a given pair of surfactants, remains to be determined as a single adjustable parameter by fit of experimental data; see Fig. 8.

It should be noted that the left-hand sides of Eqs. (21a) and (21b), which are expressing π_{el}, contain the micelle radius R_m. For a mixed micelle, R_m can be estimated by a linear mixing relation

$$R_m = (1-y_n)R_1 + y_n R_n, \qquad (46)$$

where R_1 and R_n can be estimated as the lengths of the molecules of the respective surfactants.

In addition, expressing y_n, y_1 and y_2 from Eqs. (34), (35) and (43), and substituting the results in Eq. (37), we derive:

$$\frac{1}{CMC_M} = \frac{\gamma_\pm x_1 e^{-\Phi_s} + x_{12}}{f_1 K_1^{(mic)}} + \frac{x_n}{f_n K_n^{(mic)}}, \qquad (47)$$

where CMC_M is the CMC of the mixed surfactant solution; x_1, x_{12} and x_n are the molar fractions of the respective amphiphilic components in monomeric form

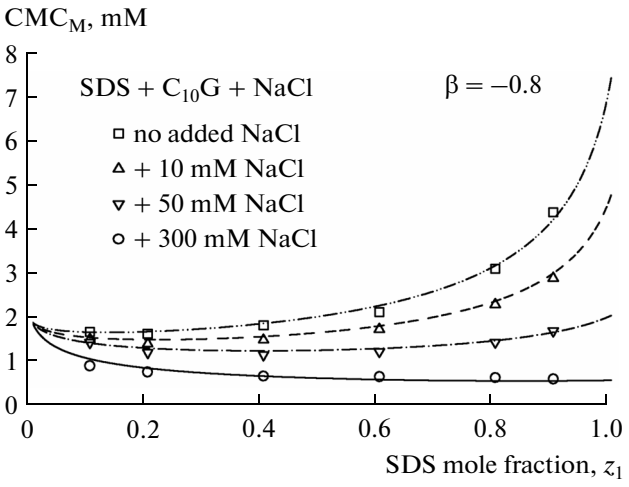

Fig. 8. Test of the theory against experimental data for mixed solutions of SDS and $C_{10}G$. Plot CMC_M vs. the SDS mole fraction z_1: the points are data from [89] at four different fixed NaCl concentrations denoted in the figure; the lines are fits to the data by the model in Section 4.1; all lines correspond to the same $\beta = -0.8$ determined from the fit [39].

($x_1 + x_{12} + x_n = 1$), which at the CMC (negligible micelle concentration) represent the composition of the solution. We have used the relation $c_i = x_i CMC_M$ (i = 1, 12, n). In many cases, the bulk molar fraction of non-ionized molecules of the ionic surfactant is very small, $x_{12} \ll 1$, so that it can be neglected in Eq. (47). x_{12} can be important for carboxylate solutions, as well as at high concentrations of added salt.

To determine the dependence of CMC_M on the composition of the micellar solution characterized by x_1, we have to solve the system of Eqs. (34)–(45). Note that in this special case $c_{mic} = 0$ and x_1 is an input parameter. Then, the number of equations has to be decreased with two. This happens by replacement of the four Eqs. (38), (39), (41) and (44) with the following two equations: $c_2 = I = c_1 + C_{salt}$. A convenient computational procedure for determining the dependence of CMC_M on x_1 is proposed in [39].

In the limiting case of two nonionic surfactants, $\Phi_s = 0$, $\gamma_\pm \approx 1$ and $x_{12} = 0$. Then, in view of Eq. (12) the expression for CMC_M in Eq. (47) reduces to the known formula for nonionic surfactants; see e.g. [72, 88].

4.2. Test of the Model against Experimental Data

In Fig. 8, the theoretical model from Section 4.1 is tested against a set of experimental data from [89] for the CMC of mixed aqueous solutions of the anionic surfactant SDS and the nonionic surfactant *n*-decyl β-D-glucopyranoside (**$C_{10}G$**) at different concentrations of added NaCl, C_{salt}. The parameters K_{St}, $K_1^{(mic)}$,

$\gamma_{0,1}$ and R_1 for SDS were taken from Table 3 in [39]. For $C_{10}G$ we have $K_n^{(mic)} = CMC_n = 2$ mM and $R_n = 2.5$ nm. All four experimental curves in Fig. 8 have been fitted simultaneously and a single value $\beta = -0.8$ has been obtained. The small magnitude and negative sign of β means that the mixture of these two surfactants is slightly synergistic. The fact that β is independent of C_{salt} means that the electrostatic double-layer interactions are adequately taken into account by Eqs. (34) and (42), so that the value of β is determined only by the non-double-layer interactions between the two surfactants, as it should be expected [39].

At the highest salt concentration, 300 mM NaCl, the bulk molar fraction of the non-dissociated SDS molecules, x_{12}, is not negligible. The data for CMC_M in Fig. 8 are plotted against the total (input) molar fraction of SDS, viz. $z_1 = x_1 + x_{12}$, which is known from the experiment.

At surfactant concentrations much above the CMC, the composition of the micelles $(y_1 + y_2, y_n)$ is practically identical with the input composition (z_1, z_n), because the amount of surfactant in monomeric form is negligible. In contrast, at the CMC the concentration of micelles is negligible, and then the input composition (z_1, z_n) becomes identical with the composition of the monomers $(x_1 + x_{12}, x_n)$. Usually x_{12} is also negligible, except at high salt concentrations or protonation of carboxylates. At the CMC, the micelle composition $(y_1 + y_2, y_n)$ is unknown, but it can be predicted by the theoretical model, together with the micelle charge and surface electric potential. Such calculations have been carried out in [39] for various mixtures of ionic and nonionic surfactants, on the basis of fits of CMC_M vs. composition dependencies, like that in Fig. 8. The main conclusions from this analysis are as follows.

The results show that the effect of counterion binding in the mixed micelles is essential only at the highest molar fractions of the ionic surfactant, $x_1 > 0.90$. At lower x_1 values, $y_2 \approx 0$. The high degree of ionization of the ionic surfactant in the mixed micelle gives rise to a relatively high micelle surface electric potential, ψ_s, even at $x_1 \approx 0.20$. The electrostatic repulsion micelle–monomer makes the incorporation of the ionic component in the micelles less advantageous than of the nonionic one. For this reason, at the CMC the micelles are enriched in the nonionic component: $y_n > y_1$ and $y_n > x_n$. This effect can be diminished if the ionic surfactant has a longer hydrophobic tail than the nonionic one.

In general, the main factors in the competition between the two surfactants to dominate the micelle are (i) the hydrophobic effect related to the length of the surfactant hydrocarbon chain, which is taken into account by the micellization constants $K_1^{(mic)}$ and $K_n^{(mic)}$, and (ii) the electrostatic potential ψ_s that diminishes the fraction of the ionic surfactant in the mixed micelles. In comparison with the effects of the micellization constants and ψ_s, the effect of the interaction parameter β represents a relatively small correction.

The analysis of experimental data for the CMC of various mixed ionic + nonionic surfactant solutions showed also that for all of them the ranges of variation of the micelle surface potential and electrostatic surface pressure are in the same range: $0 < |\psi_s| < 120$ mV and $0 < \pi_{el} < 5$ mN/m, upon variation of ionic-surfactant molar fraction in the interval $0 < x_1 < 1$.

5. SUMMARY AND CONCLUSIONS

In this article, two independent approaches for determining the aggregation number and charge of ionic surfactant micelles are presented and discussed. The *first* approach is based on the analysis of data for the stepwise thinning (stratification) of liquid films formed from micellar solutions. The height of the step yields the micelle aggregation number, N_{agg}, whereas the final thickness of the film (without micellar layers) gives the micelle charge, Z [37, 38]. The *second* approach is based on a complete system of equations (a generalized phase separation model) that describes the micelle–monomer equilibrium, including the counterion binding effect [39]. The three parameters of this model can be determined by fitting a given set of experimental data, for example, the dependence of the CMC on the salt concentration (Section 3.4). Having once determined the parameters of the model, one can further predict all properties of the micelles and monomers. The values of the micelle aggregation number, N_{agg}, and the ionization degree, α, independently determined by the two methods, are in good agreement (Fig. 6b).

In addition, using the calculated concentrations of all monomeric ionic species, we can predict also their total conductivity, which turns out to exactly coincide with the experimentally measured electrolytic conductivity of the micellar solutions in the whole range of surfactant concentrations above the CMC (Fig. 6b). In other words, the contribution of the micelles to the solution's conductivity is negligible, so that their equivalent conductance, λ_m, turns out to be practically zero.

These results on stratifying films and conductivity of micellar solutions imply that the micelles, together with their counterion atmospheres, behave as a *self-stressed* system of effective soft spheres, which are pressed against each other in the confined space of the solution, or in the liquid film. In the case of stratification (Fig. 3), the internal stress of this system opposes the external pressure and determines the thickness of the films containing micelles. In the case of conductivity measurements, the applied external electric field is weaker than the intermicellar repulsion and cannot bring the micelles into directional motion. An *experimental* indicator for the formation of such self-stressed system of charged micelles is the stratification of the

liquid films. A *theoretical* indicator is the fulfillment of the relation $d_{eff} = (c_m)^{-1/3}$, where the effective micelle diameter d_{eff} is calculated from Eq. (5) [37, 38].

The theoretical model is generalized to mixed solutions of ionic and nonionic surfactants (Section 4). The generalized model predicts the CMC of mixed surfactant solutions; the dependence of the CMC on the electrolyte concentration; the concentrations of the monomers that are in equilibrium with the micelles; the solution's electrolytic conductivity; the micelle composition, aggregation number, ionization degree and surface electric potential. The model can find applications for the analysis, interpretation and prediction of the properties of various micellar solutions of ionic surfactants and their mixtures with nonionic surfactants.

ACKNOWLEDGMENTS

The authors gratefully acknowledge the support from Unilever Research; from the FP7 project Beyond-Everest, and from COST Action CM1101.

REFERENCES

1. McBain, J.W., *Trans. Faraday Soc.*, 1913, vol. 9, p. 99.
2. *McBain, J.W.* and Salmon, C.S., *J. Am. Chem. Soc.*, 1920, vol. 42, p. 427.
3. Hartley, G.S., *Aqueous Solutions of Paraffin Chain Salts*, Paris: Hermann, 1936.
4. Vincent, B., *Adv. Colloid Interface Sci*. 2014, vol. 20, p. 51.
5. Kroflič, A., Šarac, B., and Bešter-Rogač, M., *J. Chem. Thermodynamics*, 2011, vol. 43, p. 1557.
6. Gehlen, M.H. and De Schryver, F.C., *J. Phys. Chem.*, 1993, vol. 97, p. 11242.
7. Alargova, R., Petkov, J., Petsev, D., Ivanov, I.B., Broze, G., and Mehreteab A., *Langmuir*, 1995, vol. 11, p. 1530.
8. Lang. P. and Glatter, O., *Langmuir*, 1996, vol. 12, p. 1193.
9. Petkov, J.T., Tucker, I.M., Penfold, J., Thomas, R.K., Petsev, D.N., Dong, C.C., Golding, S., and Grillo, I., *Langmuir*, 2010, vol. 26, p. 16699.
10. Bales, B.L., Messina, L., Vidal, A., Peric, M., and Nascimento, O.R., *J. Phys. Chem. B*, 1998, vol. 102, p. 10347.
11. Törnblom, M., Henriksson, U., and Ginley, M., *J. Phys. Chem.*, 1994, vol. 98, p. 7041.
12. Zana, R., *Dynamics of Surfactant Self-Assemblies*, New York: CRC Press, 2005.
13. Kamrath, R.F. and Frances, E.I., *J. Phys. Chem*. 1984, vol. 88, p. 1642.
14. Tadros, T.F., *Applied Surfactants: Principles and Applications*, Weinheim: Wiley-VCH Verlag, 2005.
15. Israelachvili, J.N., Mitchell, D.J., and Ninham, B.W., *J. Chem. Soc., Faraday Trans. 2*, 1976, vol. 72, p. 1525.
16. Missel, P.J., Mazer, N.A., Benedek, G.B., Young, C.Y., and Carey, M.C., *J. Phys. Chem.*, 1980, vol. 84, p. 1044.
17. Alargova, R.G., Danov, K.D., Kralchevsky, P.A., Broze, G., and Mehreteab, A., *Langmuir*, 1998, vol. 14, p. 4036.
18. Scrinivasan, V. and Blankstein, D., *Langmuir*, 2003, vol. 19, p. 9932.
19. Kralchevsky, P.A., Danov, K.D., Anachkov, S.E., Georgieva, G.S., and Ananthapadmanabhan, K.P., *Curr. Opin. Colloid Interface Sci.*, 2013, vol. 18, p. 524.
20. Rubingh, D.N., in *Solution Chemistry of Surfactants*, *Vol. 1*, Mittal, K.L., Ed., New York: Plenum Press; 1979.
21. Kamrath, R.F. and Frances, E.I., *Ind. Eng. Chem. Fundam.*, 1983, vol. 22, p. 230.
22. Rusanov, A.I., Shchekin, A.K., and Kuni, F.M., *Colloid J.*, 2009, vol. 71, p. 816.
23. Rusanov, A.I., *Micellization in Surfactant Solutions*, Reading: Harwood Academic, 1997.
24. Nagarajan, R., *Langmuir*, 1985, vol. 1, p. 331.
25. Rusanov, A.I., Shchekin, A.K., and Kuni, F.M., *Colloid J.*, 2009, vol. 71, p. 826.
26. Szleifer, I., Ben-Shaul, A., and Gelbart, W.M., *J. Chem. Phys.*, 1986, vol. 85, p. 5345.
27. Reif, I., Mulqueen, M., and Blankschtein, D., *Langmuir*, 2001, vol. 17, p. 5801.
28. Huibers, P.D.T., *Langmuir*, 1999, vol. 15, p. 7546.
29. Hu, J., Zhang, X., and Wang, Z., *Int. J. Mol. Sci.*, 2010, vol. 11, p. 1020.
30. Kresheck, G.C., Hamory, E., Davenport, G., and Scheraga, H.A., *J. Am. Chem. Soc.*, 1966, vol. 88, p. 246.
31. Aniansson, E.A.G. and Wall, S.N., *J. Phys. Chem.*, 1974, vol. 78, p. 1024.
32. Danov, K.D., Kralchevsky, P.A., Denkov, N.D., Ananthapadmanabhan, K.P., and Lips, A., *Adv. Colloid Interface Sci.*, 2006, vol. 119, p. 1.
33. Noskov, B.A., *Adv. Colloid. Interface Sci.*, 2002, vol. 95, p. 237.
34. Danov, K.D., Kralchevsky, P.A., Denkov, N.D., Ananthapadmanabhan, K.P., and Lips, A., *Adv. Colloid Interface Sci.*, 2006, vol. 119, p. 17.
35. Christov, N.C., Danov, K.D., Kralchevsky, P.A., Ananthapadmanabhan, K.P., and Lips, A., *Langmuir*, 2006, vol. 22, p. 7528.
36. Shchekin, A.K., Rusanov, A.I., and Kuni, F.M., *Chem. Lett.*, 2012, vol. 41, p. 1081.
37. Danov, K.D., Basheva, E.S., Kralchevsky, P.A., Ananthapadmanabhan, K.P. and Lips, A., *Adv. Colloid Interface Sci.*, 2011, vol. 168, p. 50.
38. Anachkov, S.E., Danov, K.D., Basheva, E.S., Kralchevsky, P.A., and Ananthapadmanabhan, K.P., *Adv. Colloid Interface Sci.*, 2012, vol. 183–184, p. 55.
39. Danov, K.D., Kralchevsky, P.A., and Ananthapadmanabhan, K.P., *Adv. Colloid Interface Sci.*, 2013, DOI: 10.1016/j.cis.2013.02.001.
40. Horn, R.G. and Israelachvili, J.N., *J. Chem. Phys.*, 1981, vol. 75, p. 1400.
41. Nikolov, A.D., Wasan, D.T., Kralchevsky, P.A., and Ivanov, I.B., in *Ordering and Organisation in Ionic Solutions*, Ise, N. and Sogami, I., Eds., Singapore: World Scientific, 1988.
42. Israelachvili, J.N., *Intermolecular and Surface Forces*, 3rd Ed., London: Academic Press, 2011.
43. Johonnott, E.S., *Phil. Mag*. 1906, vol. 11, p. 746.
44. Perrin, J., *Ann. Phys. (Paris)*, 1918, vol. 10, p. 160.

45. Nikolov, A.D. and Wasan, D.T., *J. Colloid Interface Sci.*, 1989, vol. 133, p. 1.

46. Nikolov A.D., Kralchevsky, P.A., Ivanov, I.B., and Wasan, D.T., *J. Colloid Interface Sci.*, 1989, vol. 133, p. 13.

47. Mitchell, D.J., Ninham, B.W., and Pailthorpe, B.A., *J. Chem. Soc., Faraday Trans. 2*, 1978, vol. 74, p. 1116.

48. Kjellander, R. and Sarman, S., *Chem. Phys. Lett.*, 1988, vol. 149, p. 102.

49. Henderson, D., *J. Colloid Interface Sci.*, 1988, vol. 121, p. 486.

50. Kralchevsky, P.A. and Denkov, N.D. *Chem. Phys. Lett.* 1995, vol. 240, p. 385.

51. Trokhymchuk, A., Henderson, D., Nikolov, A., and Wasan, D.T., *Langmuir*, 2001, vol. 17, p. 4940.

52. Christov, N.C., Danov, K.D., Zeng, Y., Kralchevsky, P.A., and von Klitzing, R., *Langmuir*, 2010, vol. 26, p. 915.

53. Denkov, N.D., Yoshimura, H., Nagayama, K., and Kouyama, T., *Phys. Rev. Lett.*, 1996, vol. 76, p. 2354.

54. Basheva, E.S., Danov, K.D., and Kralchevsky, P.A., *Langmuir*, 1997, vol. 13, p. 4342.

55. Basheva, E.S., Kralchevsky, P.A., Danov, K.D., Ananthapadmanabhan, K.P., and Lips, A., *Phys. Chem. Chem. Phys.*, 2007, vol. 9, p. 5183.

56. Scheludko, A. and Exerowa, D., *Comm. Dept. Chem. Bulg. Acad. Sci.*, 1959, vol. 7, p. 123.

57. Scheludko, A., *Adv. Colloid Interface Sci.*, 1967, vol. 1, p. 391.

58. Scheludko, A. and Platikanov, D., *Kolloid Z.*, 1961, vol. 175, p. 150.

59. Trokhymchuk, A., Henderson, D., Nikolov, A.D., and Wasan, D.T., *J. Phys. Chem. B*, 2003, vol. 107, p. 3927.

60. Jönsson, B., Broukhno, A., Forsman, J., and Åkesson, T., *Langmuir*, 2003, vol. 19, p. 9914.

61. Piech, M. and Walz, J.Y., *J. Phys. Chem. B*, 2004, vol. 108, p. 9177.

62. Tulpar, A., Van Tassel, P.R., and Walz, J.Y., *Langmuir*, 2006, vol. 22, p. 2876.

63. Klapp, S.H.L., Zeng, Y., Qu, D., and von Klitzing, R., *Phys. Rev. Lett.*, 2008, vol. 100, art. no. 118303.

64. Klapp, S.H.L., Qu, D., and von Klitzing, R., *J. Phys. Chem. B*, 2007, vol. 111, p. 1296.

65. Klapp, S.H.L., Grandner, S., Zeng, Y., and von Klitzing, R., *J. Phys.-Condensed Matter*, 2008, vol. 20, art. no. 494232.

66. Zeng, Y., Grandner, S., Oliveira, C.L.P., Thünemann, A.F., Paris, O., Pedersen, J.S., Klapp, S.H.L., and von Klitzing, R., *Soft Matter*, 2011, vol. 7, p. 10899.

67. Beresford-Smith, B. and Chan, D.Y.C., *Faraday Discuss. Chem. Soc.*, 1983, vol. 76, p. 65.

68. Beresford-Smith, B., Chan, D.Y.C., and Mitchell, D.J., *J. Colloid Interface Sci.*, 1985, vol. 105, p. 216.

69. Pashley, R.M. and Ninham, B.W., *J. Phys. Chem.*, 1987, vol. 91, p. 2902.

70. Richetti, P. and Kékicheff, P., *Phys. Rev. Lett.*, 1992, vol. 68, p. 1951.

71. Toshev, B.V. and Ivanov, I.B., *Colloid. Polym. Sci.*, 1975, vol. 253, p. 558.

72. Bourrel, M. and Schechter, R.S., *Microemulsions and Related Systems. Formulation, Solvency, and Physical Properties*, New York: Marcel Dekker, 1988.

73. Robinson, R.A. and Stokes, R.H., *Electrolyte Solutions*, London: Butterworths, 1959.

74. Prigogine, I. and Defay, R., *Chemical Thermodynamics*, London: Longmans, Green and Co., 1954.

75. Winstein, S., Clippinger, E., Fainberg, A.H., Heck, R., and Robinson, G.C., *J. Am. Chem. Soc.*, 1956, vol. 78, p. 328.

76. Mitchell, D.J. and Ninham, B.W., *J. Phys. Chem.*, 1983, vol. 87, p. 2996.

77. Evans, E.A. and Skalak, R., *CRC Crit. Rev. Bioeng.*, 1979, vol. 3, 181.

78. Ohshima, H., Healy, T.W., and White, L.R., *J. Colloid Interface Sci.*, 1982, vol. 90, p. 17.

79. Corrin, M.L. and Harkins, W.D., *J. Am. Chem. Soc.*, 1947, vol. 69, p. 683.

80. Mukhim, T. and Ismail, K., *J. Surf. Sci. Technol.*, 2005, 21, 113.

81. Corrin, M.L., *J. Colloid Sci.*, 1948; vol. 3, p. 333.

82. Harned, H.S. and Owen, B.B., *The Physical Chemistry of Electrolytic Solutions*, 2nd Ed. New York: Reinhold Publishing Corp., 1950.

83. Kralchevsky, P.A., Boneva, M.P., Danov, K.D., Ananthapadmanabhan, K.P., and Lips, A., *J. Colloid Interface Sci.*, 2008, vol. 327, p. 169.

84. Ravdel, A.A. and Ponomareva, A.M., *Concise Handbook of Physicochemical Quantities*, 8th Ed. Leningrad: Khimiya, 1983 [in Russian].

85. Lide, D.R., Ed., *CRC Handbook of Chemistry and Physics*, 89th Ed. New York: CRC Press, 2008.

86. Moroi, Y. and Yoshida, N., *Langmuir*, 1997, vol. 13, p. 3909.

87. Hill, T.L., *An Introduction to Statistical Thermodynamics*. New York: Dover, 1987.

88. Tzocheva, S.S., Kralchevsky, P.A., Danov, K.D., Georgieva, G.S., Post, A.J., and Ananthapadmanabhan, K.P., *J. Colloid Interface Sci.*, 2012, Vol. 369, p. 274.

89. Bergström, M., Jonsson, P., Persson, M., and Eriksson, J.C., *Langmuir*, 2003, vol. 19, p. 10719.